Competition between Harmonic Cyclotron Maser Interactions in the Terahertz Regime

S. H. Kao,[1,2] C. C. Chiu,[1] K. F. Pao,[1] and K. R. Chu[1]

[1]*Department of Physics, National Taiwan University, Taipei 106, Taiwan*

[2]*Department of Physics, National Tsing Hua University, Hsinchu 300, Taiwan*

(Received 7 June 2011; published 19 September 2011)

Cyclotron harmonic interactions are a key physics issue of critical importance to the generation of terahertz radiation via the electron cyclotron maser instability for practical magnetic field strengths. We present an inherent mechanism, as well as a deciding factor, which governs the competition between low- and high-harmonic interactions. Multimode simulations reveal the physical process in which a significant advantage develops for the lower-harmonic interaction, which eventually dominates in the fully nonlinear stage. The results also suggest a start-up scenario for persistent higher-harmonic operation.

DOI: 10.1103/PhysRevLett.107.135101 PACS numbers: 84.40.Ik, 84.40.Fe

The gyrotron, a device based on the electron cyclotron maser instability [1,2], possesses the capability of generating unprecedented power levels in the millimeter and submillimeter wave regimes with a myriad of novel applications [3]. It is also an intriguing nonlinear system in that mode competition in different embodiments follows entirely different rules and each exhibits rather unique characteristics. In the most prevalent version, the gyrotron oscillator (gyromonotron), all modes have similar spatial profiles and evolve from comparable noise levels; hence, the lowest oscillation threshold becomes a dominant advantage. An early starting mode during the rise of the beam pulse tends to suppress all parasitic modes [4,5] in the absence of some kind of external control such as a drive signal [6]. By comparison, axial modes of the gyrotron backward-wave oscillator are characterized by an asymmetric field profile [7]. Thus, the fundamental mode which peaks upstream has an overwhelming advantage and will eventually suppress any early starting mode with a less favorable profile [7]. For the gyrotron traveling-wave amplifier, on the other hand, the amplifying mode has a significantly larger initial field strength due to the drive signal. Thus, as it grows, the associated beam perturbations will appear as deleterious velocity and energy spreads to all other modes and thereby increase their oscillation thresholds as a result [1,8].

In recent years, there has been worldwide interest in terahertz (THz) sources and, in particular, the THz gyrotrons [9–18]. The latter device represents a unique approach to produce coherent THz radiation at moderate to high power levels. The lack of practical THz sources at these power levels has hampered applications such as high data rate communications, advanced radar, remote sensing, imaging, and security screening. This has in turn brought into focus the critical advantage of harmonic interactions, which reduce a 40-T field requirement at 1 THz by a factor equal to the cyclotron harmonic number. However, harmonic interactions are much weaker and, despite their importance for THz wave generation, the competition process between low- and high-harmonic modes has thus far received very little attention. For example, questions may arise as to whether and to what extent the disadvantage of weak interaction can be overcome by an early start of the higher-harmonic mode. At THz frequencies, the issue of harmonic excitation is further compounded by the desirability of a high-order (spatial) mode in order to reduce wall losses and fabrication difficulties. Consequently, a theoretical investigation of these issues is an essential first step to the implementation of the electron cyclotron maser instability for THz radiation in a practical magnetic field.

In this Letter, we begin by elucidating a physical mechanism which governs the competition between modes of different cyclotron harmonics. The intrinsic nature of this mechanism, which favors the lower-harmonic interaction, is demonstrated in a representative example. On the other hand, we demonstrate that, through the external arrangement of a proper start-up process, it is possible to give the higher-harmonic interaction a considerable competitive advantage. General trends are predicted for various modes over a broad tuning range up to the THz regime, and results agree well with available experimental data.

Nonlinear implication of the harmonic interaction strength.—The interaction strength between an electron (guiding center at r_c and a Larmor radius of r_L) and a TE_{mn} mode at the sth cyclotron harmonic is given by the coupling coefficient H_{sm} [1]:

$$H_{sm} = J_{s-m}^2(k_{mn} r_c) J_s'^2(k_{mn} r_L),$$

where J_n is the Bessel function of order n, $k_{mn} = x_{mn}/r_w$, r_w is the wall radius, and x_{mn} is the nth nonzero root of $J_s'(k_{mn} r_L) = 0$. Figure 1 shows the dependence of H_{sm} (through the second factor) on s and r_L. It is seen that H_{sm} decreases sharply with an increasing s; however, this can be compensated with a large r_L (the electron energy). Consequently, gyrotrons based on harmonic interactions are relatively scarce [9,11,14,15] in spite of a long history of research [19–21].

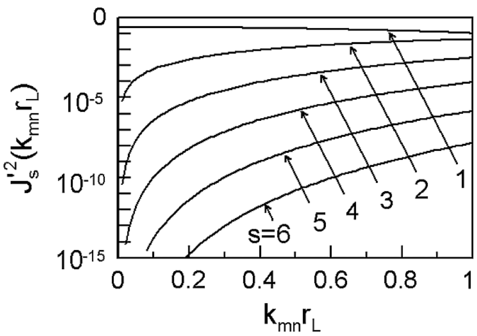

FIG. 1. Dependence of the beam-wave coupling strength on the cyclotron harmonic number s and electron Larmor radius r_L.

There is, however, another important implication in the sensitivity of H_{sm} to r_L for $s > 1$. That is, in the nonlinear stage, the harmonic interaction strength becomes much weaker for the favorable electrons (which lose energy to the wave) and much stronger for the unfavorable electrons. Furthermore, the nonlinear variation in H_{sm} is more pronounced for a higher s, which gives the lower-harmonic mode an inherent advantage over the high-harmonic mode. The fundamental-harmonic mode ($s = 1$), with the highest H_{sm} and least sensitivity to r_L, clearly possesses a tremendous advantage (which is not insurmountable, as will be shown). These considerations form the basis of the current study.

Model, assumptions, and numerical methods.—For the purpose of comparison, we adopt the configuration [Fig. 2(a)] of the Fukui THz gyrotron [9] and assume a rise-time profile of the electron beam as shown in Fig. 2(b). A stationary code [1] is used to evaluate the oscillation threshold of a single mode. A multimode, time-dependent, particle-in-cell code [7] is employed for the mode competition study. Both codes assume the transverse field structure of the cold TE mode, and all solutions are obtained under the assumption of outgoing-wave boundary conditions.

Detailed analysis of a representative case.—Figure 3(a) shows the start-oscillation currents (I_{st}) of possible modes calculated for the parameters of the Fukui experiment [9]: V_b (beam voltage) $= 30$ kV, α $(= v_\perp/v_\parallel) = 1.1$, $r_c = 0.35$ mm, and $\Delta v_z/v_z$ (electron velocity spread) $=$ 10%. The data are displayed in a narrow (but representative) magnetic field range of 16.6 T $< B <$ 16.9 T. For a multimode simulation of the competition between the TE_{89} ($s = 2$) and TE_{35} ($s = 1$) modes, the magnetic field was set at $B = 16.76$ T so that the TE_{89} mode has a lower I_{st} (0.32 A) than that of the TE_{35} mode (0.65 A).

Figure 3(b) displays the time-frequency analysis of the output power (P_{out}) over a time period during which I_b builds up from 0 to 10 A (peak value). As I_b rises above the I_{st} of the TE_{89} ($s = 2$) mode, P_{out} (of TE_{89}) starts to grow to a level sufficient to suppress the TE_{35} ($s = 1$) mode up to $14.7xI_{st}$ of the TE_{35} mode. This indicates a very strong presence of the early starting harmonic mode. Then, as I_b

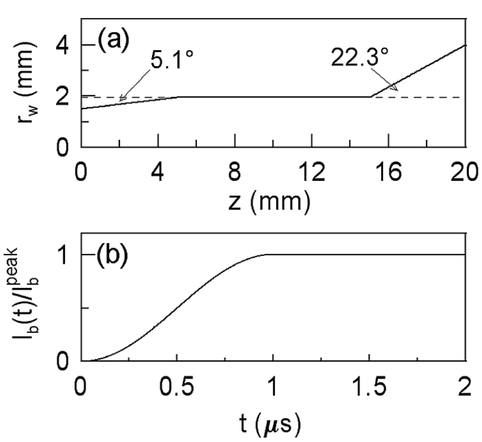

FIG. 2. (a) Configuration and dimensions of the gyrotron interaction structure under study. (b) Rise-time profile of the beam current.

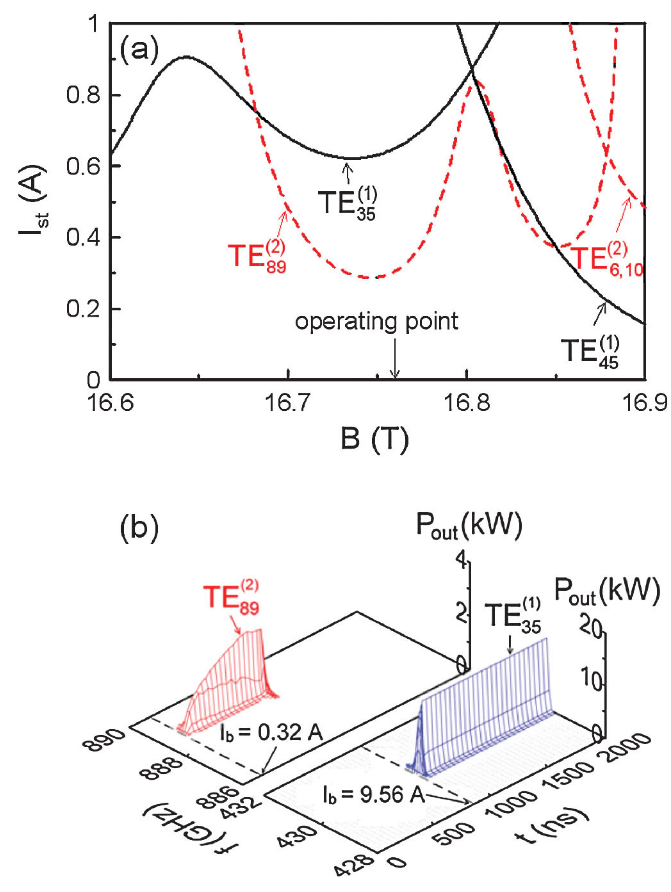

FIG. 3 (color). (a) I_{st} vs B for $V_b = 30$ kV, $\alpha = 1.1$, $r_c = 0.35$ mm, and $\Delta v_z/v_z = 10\%$. The superscript gives the cyclotron harmonic number s. (b) Time-frequency analysis of the output power showing the competition between the TE_{89} ($s = 2$) and TE_{35} ($s = 1$) modes. $B = 16.76$ T and I_b (peak) $= 10$ A.

rises further, the TE_{35} ($s = 1$) mode suddenly takes over and completely suppresses the (already saturated) TE_{89} mode on a nanosecond time scale. The details and the reason for this are discussed in the following figure.

Figure 4 plots the evolution of the beam-wave coupling coefficient H_{sm} along the z axis at $I_b = 10$ A for an ensemble of individual electrons in the cyclotron phase space. For the TE_{35} ($s = 1$) mode [Fig. 4(a)], H_{sm} remains relatively constant as is expected from Fig. 1 ($s = 1$). However, for the TE_{89} ($s = 2$) mode [Fig. 4(b)], H_{sm} increases by as much as 50% for electrons in the energy-gaining phase, while it decreases by as much as 56% for those in the energy-losing phase. This is extremely unfavorable for the $s = 2$ interaction. On the other hand, the well-established TE_{89} ($s = 2$) oscillation tends to maintain a strong presence. Thus, the entire process becomes a competition between these two opposing factors. It eventually ends with the complete suppression of the TE_{89} mode but only at an I_b much higher than the I_{st} of the TE_{35} mode.

Further verification and general trend over the full tuning range.—Figures 3 and 4 describe a representative case of low- and high-harmonic competition although there is only a narrow window in the I_b-B parameter space for the early start of the $s = 2$ modes. Figure 5 shows a simulated mode chart for different I_b over a broad range of B. The data for I_b (peak) = 1 A reproduce very closely the observed mode chart in Fig. 9 of Ref. [9]. However, as I_b increases [Figs. 5(b)–5(d)], the window for $s = 2$ operation narrows and eventually disappears at I_b (peak) = 15 A [22].

In conclusion, we have elucidated the competition between low- and high-harmonic electron cyclotron maser interactions, a process radically different from those reported previously. In spite of its much weaker interaction strength, the high-harmonic mode is shown to have a strong staying power once it is excited early in the beam pulse. This suggests a promising start-up scenario for the harmonic generation of THz radiation. However, the competition process is eventually governed by an inherent mechanism in favor of the lower-harmonic mode, which leads to the sudden and complete suppression of the higher-harmonic mode at a sufficiently high beam current. The results match closely with, as well as provide

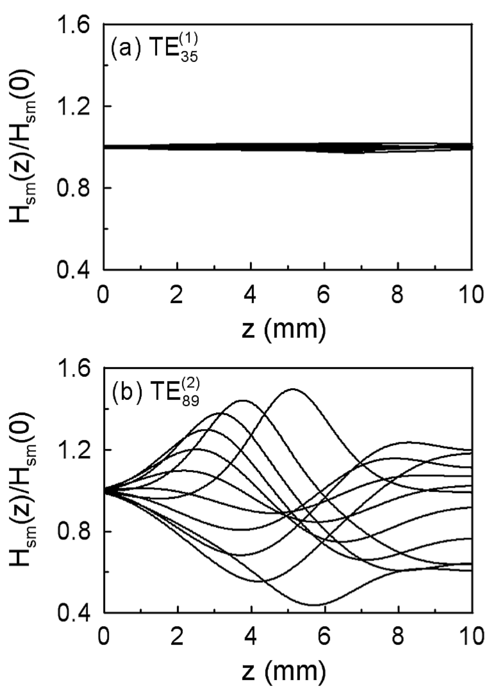

FIG. 4. H_{sm} (normalized to the initial value) versus z for (a) the TE_{35} ($s = 1$) mode and (b) the TE_{89} ($s = 2$) mode. The parameters are the same as in Fig. 3.

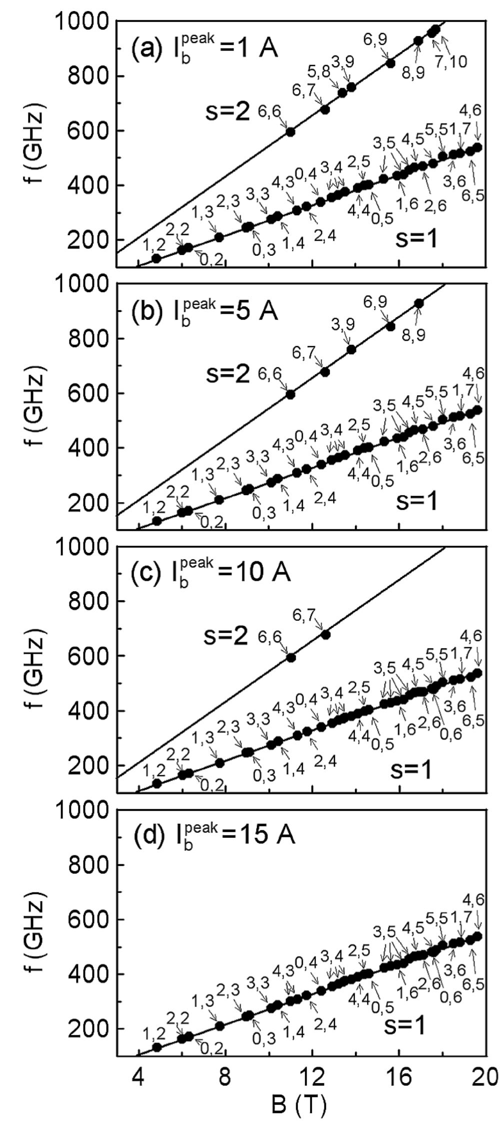

FIG. 5. Mode charts in a broad tuning range of B up to the THz frequency. (a) I_b (peak) = 1 A; (b) I_b (peak) = 5 A; (c) I_b (peak) = 10 A; (d) I_b (peak) = 15 A.

a physical interpretation of, the measurements in Ref. [9]. General trends beyond available experimental data are also predicted, which provide a road map to harmonic THz gyrotron implementation.

This work was sponsored by the National Science Council, Taiwan, and the National Taiwan University. The authors are grateful to the National Center for High Performance Computing for providing generous computing time.

[1] K. R. Chu, Rev. Mod. Phys. **76**, 489 (2004).
[2] G. S. Nusinovich, *Introduction to the Physics of Gyrotrons* (Johns Hopkins University, Baltimore, 2004).
[3] *Applications of High Power Microwaves*, edited by A. V. Gaponov-Grekhov and V. L. Granatstein (Artech House, Norwood, MA, 1994).
[4] K. E. Kreischer and R. J. Temkin, Phys. Rev. Lett. **59**, 547 (1987).
[5] G. S. Nusinovich, IEEE Trans. Plasma Sci. **27**, 313 (1999).
[6] G. S. Nusinovich, O. V. Sinitsyn, and T. M. Antonsen, Jr., Phys. Rev. Lett. **98**, 205101 (2007).
[7] K. F. Pao, T. H. Chang, C. T. Fan, S. H. Chen, C. F. Yu, and K. R. Chu, Phys. Rev. Lett. **95**, 185101 (2005).
[8] L. R. Barnett, L. H. Chang, H. Y. Chen, K. R. Chu, W. K. Lau, and C. C. Tu, Phys. Rev. Lett. **63**, 1062 (1989).
[9] T. Idehara, T. Saito, I. Ogawa, S. Mitsudo, Y. Tatematsu, La Agusu, and H. Mori, and S. Kobayashi, Appl. Magn. Reson. **34**, 265 (2008).
[10] M. Yu. Glyavin, A. G. Luchinin, and G. Yu. Golubiatnikov, Phys. Rev. Lett. **100**, 015101 (2008).
[11] T. Notake, T. Saito, Y. Tatematsu, A. Fujii, S. Ogasawara, La Agusu, I. Ogawa, T. Idehara, and V. N. Manuilov, Phys. Rev. Lett. **103**, 225002 (2009).
[12] V. Bratman, M. Glyavin, T. Idehara, Y. Kalynov, A. Luchinin, V. Manuilov, S. Mitsudo, I. Ogawa, T. Saito, Y. Tatematsu, and V. Zapevalov, IEEE Trans. Plasma Sci. **37**, 36 (2009).
[13] Y. M. Shin, L. R. Barnett, D. Gamzina, N. C. Luhmann, Jr., M. Field, and R. Borwick, Appl. Phys. Lett. **95**, 181505 (2009).
[14] V. L. Bratman, Yu. K. Kalynov, and V. N. Manuilov, Phys. Rev. Lett. **102**, 245101 (2009).
[15] A. C. Torrezan, S. T. Han, I. Mastovsky, M. A. Shapiro, J. R. Sirigiri, R. J. Temkin, A. B. Barnes, and R. G. Griffin, IEEE Trans. Plasma Sci. **38**, 1150 (2010).
[16] I. V. Bandurkin, Yu. K. Kalynov, and A. V. Savilov, Phys. Plasmas **17**, 073101 (2010).
[17] A. W. Fliflet, M. K. Hornstein, and S. H. Gold, IEEE Trans. Plasma Sci. **39**, 1061 (2011).
[18] G. S. Nusinovich, R. Pu, T. M. Antonsen, O. V. Sinitsyn, J. Rodgers, A. Mohamed, J. Silverman, M. Al-Sheikhly, Y. S. Dimant, G. M. Milikh, Gennady M. Milikh, M. Yu. Glyavin, A. G. Luchinin, E. A. Kopelovich, and V. L. Granatstein, J. Infrared Millimeter Terahertz Waves **32**, 380 (2010).
[19] D. S. Furuno, D. B. McDermott, C. S. Kou, N. C. Luhmann, Jr., and P. Vitello, Phys. Rev. Lett. **62**, 1314 (1989).
[20] Q. S. Wang, D. B. McDermott, and N. C. Luhmann, Jr., Phys. Rev. Lett. **75**, 4322 (1995).
[21] V. L. Bratman, A. E. Fedotov, Y. K. Kalynov, V. N. Manuilov, M. M. Ofitserov, S. V. Samsonov, and A. V. Savilov, IEEE Trans. Plasma Sci. **27**, 456 (1999).
[22] This trend also agrees with the unpublished Fukui data [T. Idehara (private communication)].